Proceedings of the Sixth International Conference on
Railway Technology: Research, Development and Maintenance
Edited by: J. Pombo
Civil-Comp Conferences, Volume 7, Paper 3.14
Civil-Comp Press, Edinburgh, United Kingdom, 2024
ISSN: 2753-3239, doi: 10.4203/ccc.7.3.14

Experimental-Numerical Analysis of High-Speed Train Slipstream in Open Air and Confined Spaces

S. Negri, G. Tomasini, P. Schito, D. Rocchi, F. F. Semeraro and C. E. Araya Reyes

Department of Mechanical Engineering, Politecnico di Milano, Italy

Abstract

The study addresses the aerodynamic impact of train slipstreams, crucial for passenger and worker safety. While previous research has extensively examined open-field scenarios, limited attention was given to slipstream development in confined spaces. In literature the differences between slipstream in open fields and tunnels were observed, highlighting the role of infrastructure parameters in airflow restriction during train passage, mainly through numerical simulations; however, the computational fluid dynamics analysis with only few experimental data available remains challenging. To bridge this gap and fully understand the slipstream differences in open air and tunnels, the results from a full-scale experimental campaign on an Italian railway line for analyzing airflow in different environments were considered. This paper presents findings exploiting data from the campaign, comparing slipstream features in tunnels and open spaces, thanks to air speed measurements collected in both environments simultaneously, considering geometrical effects given by asymmetrical tunnel shapes. In the second part of the work a computational fluid dynamics model is employed for a deeper analysis of the velocity field in tunnels, providing insights into the complex

interaction between train and tunnel geometry and give the basis to further work exploiting the capability of the computational fluid dynamics model to reproduce the slipstream stochastic nature.

Keywords: high-speed train, aerodynamics, slipstream, full-scale, numerical analysis, open air, tunnel.

1 Introduction

The train slipstream, crucial for railway vehicle aerodynamics study, directly impacts passenger and track worker safety due to high transit speeds generating potentially dangerous gusts. While extensive analyses have been conducted in open fields, limited research focuses on the slipstream's development in confined spaces, emphasizing the need for comprehensive research in such environments.

Previous studies, with full-scale tests [1], moving model analyses [2]; [3] and numerical simulations [4] primarily focused on open-field scenarios, however a limited attention has been given to the slipstream's development in confined spaces, where interactions with enclosure geometry can result in additional speed-up effects [5]. Significant differences between the slipstream generated in open field and in confined spaces are present, since the latter depends not only on the train parameters but also on those related to the infrastructure, which presents a key role for the air flow restriction during the train passage. Nevertheless, to the best of the authors' knowledge, the literature offers only a limited number of analyses based on full-scale measurements performed on conventional railway lines, necessary to assess with statistical significance, i.e. with an adequate number of train passages, a stochastic phenomenon as the train slipstream. Most of existing works mainly deal with computational fluid dynamics, which application to the railway environment is extensively used for the typical issues related to high-speed trains aerodynamics [6]. However, the predominant focus on numerical simulations in current research poses a challenge, as validation with a few available experimental data is not trivial.

This work aims to use data coming from a full-scale experimental campaign at the Italian railway line ([5]), whose setup is recalled in Section 2, to study the main features and differences of the slipstream measured inside the tunnel and in open spaces, taking into account the differences in the slipstream trend and maximum peaks recorded in the two tracks directions, due to the non-symmetrical shape of the tunnel (Section 3). Conducting full-scale measurements in both settings at the same time is not usually possible, often focusing on either flow and pressure fields in a single space; conversely, during the campaign the air speed measurements were carried out for the same collections of train passages in both environments, providing comprehensive data for a direct slipstream comparison. This work aims to assess phenomena in both environments, including the tunnel-specific piston effect and overall airflow characteristics resulting from the train's passage through the platforms. In the second part of the research, in Section 4, a CFD model based on the unsteady Reynolds-averaged

Navier-Stokes (URANS) approach is developed considering the real tunnel and train geometries, showing the model capability to reproduce the characteristics features of the slipstream behavior in confined spaces. The numerical model is then used to analyze the complete velocity field in tunnel and obtain and compare the slipstream measurements on specific locations in the platform region. Finally, in Section 5, the conclusions and an overview of the further work which will be done are summarized.

2 Experimental setup and post processing

A full-scale experimental campaign was performed on the Italian railway line ([5]), to measure the air speed generated by different train types at their passage. The site chosen for the measurement stations included two different areas: a platform zone located inside a railway tunnel and an open air section situated at the tunnel exit.

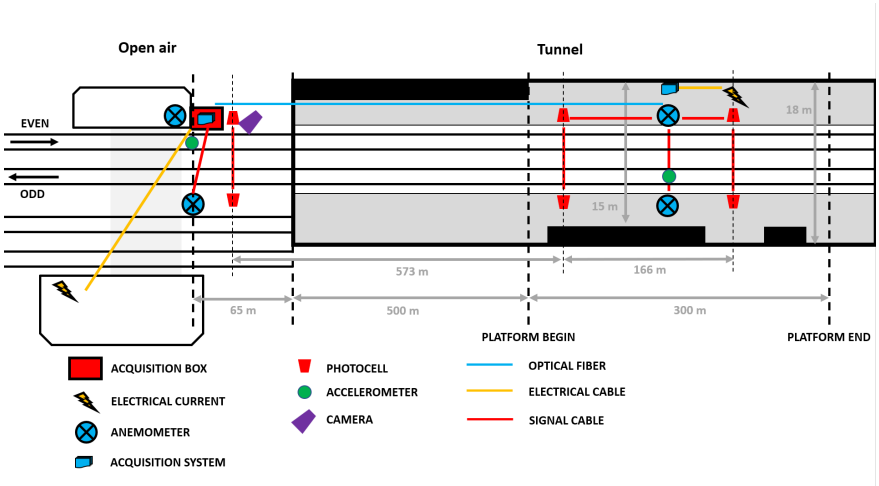

Figure 1: Experimental set-up: open air and internal measurement stations for even and odd track directions.

In Figure 1 it is shown the experimental setup adopted during the experimental campaign to measure the train slipstream. The instruments used during the campaing to acquire the wind data and characterize the train passages included four 3-Axis ultrasonic anemometers, placed along the line in open air and in the tunnel (Figure 2), 1.2 m high from the platform (according to the TSI standard ([7])) and at 2.5 m (the closest allowed position for the passengers) and 3 m from the track centres, photocell gates and accelerometers inside the tunnel and in open air to estimate the train's speed and length and to trigger the acquisition system and a camera, fixed outside the tunnel on a catenary pole, to allow a precise train recognition.

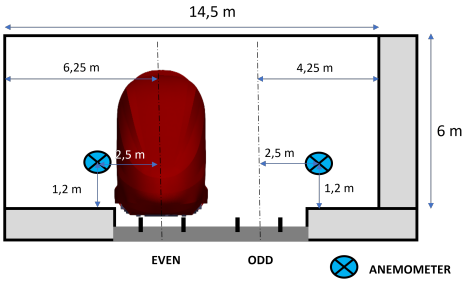

Figure 2: Scheme of tunnel cross section at the anemometer's position in the tunnel platform.

To enhance the train and tunnel characterization, Table 1 incorporates details on train length, car count, cross-sectional area, and blockage ratio ($A_{\text{train}}/A_{\text{tunnel}}$), accounting for the fact that the tunnel's cross-section in the measurement zone corresponds to 84 m^2.

Table 1: Train length, quantity of coaches, frontal area, and the blockage ratio for high-speed trains.

Train type	**Train length [m]**	**N. cars**	**Train cross sectional area**	**Blockage ratio** (Atr/Atu)
ETR1000	202	8	10.9	0.13012

Given that the slipstream is an intrinsically unsteady phenomenon, the air measurements obtained with the experimental campaign should be post-processed in order to analyse the main flow characteristics and to compare the different train behavior inside and outside the tunnel ([8], [9]). In the following sections, the slipstream phenomenon will be analysed by plotting the ensemble means of the wind velocity acquisitions for many passages of the same train type, performing the ensemble averaging technique. The wind histories were aligned with space $x = 0\ m$ to a common position, which is considered as the train nose passage in front of the anemometers; then, the mean and standard deviation values, considering the velocity values at the same spatial position, were calculated. The measured vertical velocity components were small and only the longitudinal component of the horizontal velocities will be shown in the next sections, since they can be considered the most significant contribution to the slipstream wind.

Moreover, as the slipstream wind velocities depend on the train speed and observing that trains do not travel exactly at the same velocity in the railway line (in the tunnel as in open air) the train speed effect on the air flow characteristics is removed by scaling the air speed to a reference train velocity (V_{ref}), as reported in Eq. (1) where U_{air} represents the air speed measured in the train direction and V_{train} is the train traveling speed estimated for each specific passage.

$$U_x = \frac{U_{\text{air}}}{V_{\text{train}}} \cdot V_{\text{ref}} \tag{1}$$

For the experimental data analysis, a specific reference speed is selected for the train type analyzed (high-speed train) by considering the average of the traveling speed inside the tunnel measured during the experimental campaign for the train groups analyzed, which correspond to 120 km/h. As shown in [10] and [2], the measured slipstream velocities present a linear relationship with respect to train speed for velocity data, therefore the scaling approach employed in this study can be regarded as an appropriate methodology.

3 Analysis of experimental data

The study of the slipstream phenomenon includes two locations: the railway tunnel and an open space near the tunnel exit. Air speed measurements were conducted in both environments for each train passage, ensuring comprehensive information for a direct comparison of slipstreams. The ability to compare not only identical train types but also directly assess the same train passages inside and outside the tunnel constitutes a fundamental aspect of this analysis. Full-scale measurements in two separate environments and at the same time are rarely achievable, usually focusing on the measure of the flow and pressure fields in a single space or directly on the train surface. The analysis in this paper includes all the phenomena which develop in the two spaces considering, i.e. the so-called piston effect - only present when trains are traveling in tunnels - and the overall air flow characteristics caused by the train passing over the measurement zone. Regarding the upcoming sections, the examination of experimental data is divided in two parts: in Section 3.1 the comparison between the slipstream measured inside and outside the tunnel at the passage of ETR1000 high-speed trains is performed, while in Section 3.2 the influence of the platform geometry, considering the two track directions inside and outside of the tunnel, is described. The main characteristics of all the train groups considered in the study are reported in Table 2.

Train type	**Train length [m]**	**Number of passages**	**Track direction**	**Measurement position from track center [m]**	**Reference speed [km/h]**
ETR1000	202	19	Even	2.5	120
ETR1000	202	32	Odd	2.5	120

Table 2: Open air and confined space comparison, train groups characteristics.

3.1 Characteristics flow features in open air and confined space

The first part of the analysis concerns the comparison between the slipstream profiles generated in open field and in tunnel for the high-speed trains. Figure 3 shows the ensemble mean profiles of the longitudinal air speed component measured for trains on the even track direction, inside and outside of the tunnel.

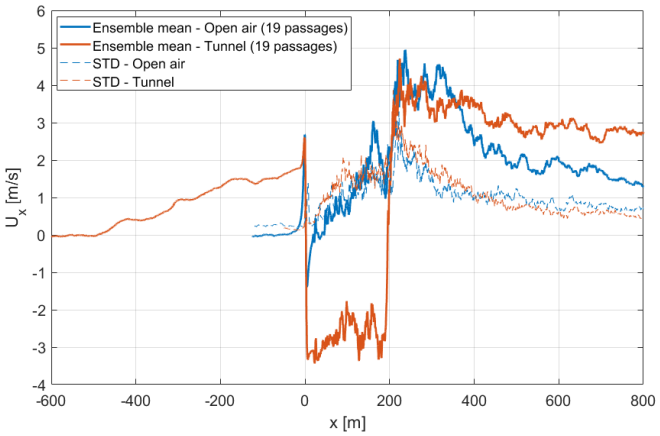

Figure 3: Open air/confined space comparison on the even track. On x axis: train nose position from anemometer, on y axis: ensemble mean and standard deviation (STD) of longitudinal air speed.

The results show that the air flow develops differently inside the tunnel with respect to the open field, with specific characteristics for each environment. The differences between the slipstream profiles are now analyzed in the three main slipstream regions, delimited by the train nose, body and tail passage. In the upstream/nose region, the first difference which could be noted is the presence of the flow speed increase during the tunnel passage, related to the piston effect, starting about 500 m before the train nose passing (distance between the tunnel entrance and the measurement point), while in the open air the flow remains in static conditions until the train nose passage in front of the measurement position. As studied in [5], the flow velocity preceding the passage of a train, induced by the piston effect, primarily depends on the train's volume. Every train entering the tunnel exhibits a nearly linear rise in air velocity before its passage, attaining higher speeds for longer trains characterized by a less a erodynamic shape.

Regarding the boundary layer region, a completely different behavior is highlighted in open air and in tunnel: while in non-confined conditions the flow assumes negative velocity just after the train nose passage (due to the generation of a pressure wave caused by the nose passage itself) and then it assumes positive increasing values up to the train tail passing, in confined space the presence of a prolonged back flow is evident. When the train reaches the anemometers position, a reversed flow is measured because of the piston effect: the train, acting as a piston in the tunnel, creates a counter flow in the annular zone between the train and the tunnel walls, where the air is pushed to flow in the opposite direction with respect to the train movement. Finally the third zone, the wake region, can be analyzed for high-speed trains: considering the even track direction, the peaks measured in open air and in confined space are generated right after the train tail passage, in the near wake zone, and show similar maximum values. From the data, it can be inferred that in the tunnel, considering the even track direction, the air confinement does not generate stronger velocity gusts in the wake. However, two main considerations can be made: when referring to real tunnels, the

cross-section geometry can vary along the tunnel length (as it is for the current tunnel, as shown in Figure 1 scheme) and the flow is perturbed by this changes, as will be described in 3.2. Secondly, even though the maximum peaks recorded in open air and tunnel have similar amplitudes, the effective velocity variation felt by people in the platform in confined spaces is greater due the presence of the back flow region, while in open air the air speed is increasing in a monotonous trend up to the tail related peak.

Finally, Figure 3 shows also the standard deviation profiles for each group, from which it can be inferred that the stochastic distribution of the slipstream is comparable between open and closed environments, proving the validity of the ensemble averaging technique also for train passages in tunnel.

3.2 Platform effect in tunnel

Dealing with confined spaces, the influence of the local infrastructure geometry and of the measurement position on the pressure waves and velocity field generated at the train passage is known ([11], [12]). Therefore, to understand whether more or less critical conditions are present in the tunnel in terms of maximum air speed, it is necessary to consider probes placed at different tunnel locations. In this section, the analysis focuses on the slipstream produced by trains traveling in the two opposite directions, i.e. even and odd track directions. Because of the non-symmetrical tunnel geometry near the platorm area (Figure 1), the influence of the measurement location is addressed and the main conclusion are drawn for the high-speed train passages. The ensemble mean and standard deviation of the air velocity is reported in Figure 4, where in (a) are shown the profiles for the even track direction and in (b) for the odd track direction in open air and in tunnel.

From these profiles, it is noted the most critical effect of the tunnel contrainment on the passages on the odd track, highlighting greater velocity peaks on tunnel side than in open field. The profiles show that the velocity maxima are generated in the near wake zone for both the track directions, but the trend developed on the odd track presents a faster velocity growth, already from the boundary layer area, than on the even track. This difference can be appreciated from about 50 m after the train nose passage and is carried on until the tail passage, causing higher maximum slipstream velocities on the tunnel narrower side with respect to the ones measures in open air. The results highligth the presence of the most critical condition in a specific zone of the tunnel, caused by its local geometry; on the even track side, in which strong shape variations are not present and which has a wider platform, the air speed maxima between open air and confined space passages are comparable.

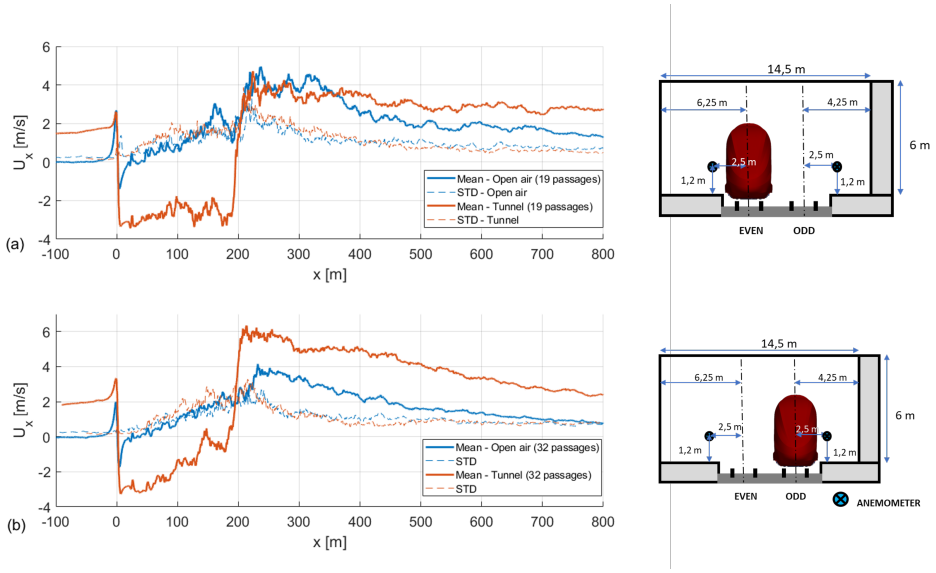

Figure 4: Open air/confined space comparison for high-speed trains (L=202m). In (a) passages on the even track direction, in (b) passages on the odd track direction. On x axis: train nose position from anemometer, on y axis: ensemble mean and standard deviation (STD) of longitudinal air speed.

4 Numerical analysis

To reproduce the slipstream phenomenon with numerical models, a CFD analysis is performed in open air and in the railway tunnel used to perform the experimental analaysis described in the previous sections. The numerical setup should be able to reproduce the full-scale ETR1000 high-speed train running at the operational speed in the line, i.e. 120 km/h. The simulations are made by using the 3D, unsteady Reynolds-averaged Navier-Stokes (URANS) approach, which has proven to be affordable and robust in modelling the slipstream around a moving train [6], using the PIMPLE algorithm. The flow incompressibility assumption is made since the considered train speed in tunnel was relatively low (Mach number $<<$ 0.3). The detailed description of the simulations of the train passage in confined spaces is reported in Section 4.1 and Section 4.2, respectively.

4.1 Setup

The computational domain was discretized by using the finite volume method in OpenFOAM, reproducing open air conditions and the real railway tunnel geometry. The dimensions of the numerical domain are selected to avoid far field effects and are reported, along with the boundary conditions, in Figure 5.

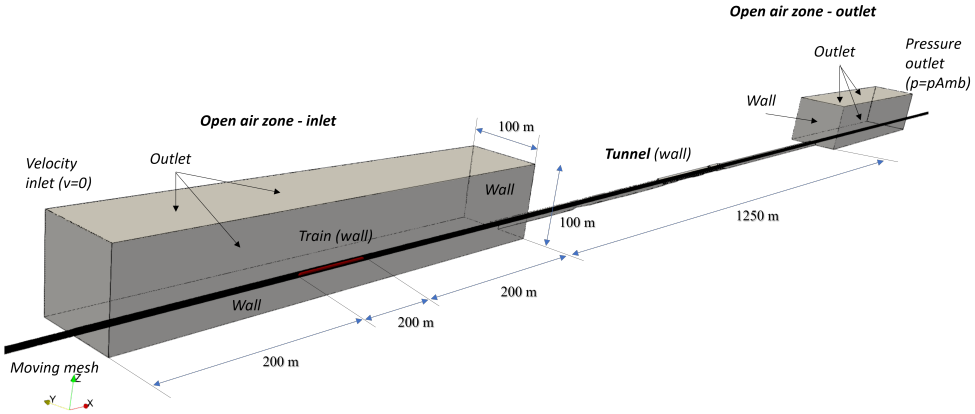

Figure 5: Computational domain and boundary conditions

The ETR1000 high-speed train was considered for the study because of its fixed configuration with 8 cars and 202 m length, which was the same configuration recorded during the experimental campaign. The train it was inserted within a sliding mesh region to guarantee realistic conditions of the flow in the simulation, necessary for the reproduction of the flow within confined spaces. As wall function approach was selected to model the near wall regions, the grid size was set, following a mesh independence study, and refinement boxes around the train and layer cells were employed around the train surface to achieve the correct value for $Y+$. The boundary conditions were set as fixed velocity (equal to 0 m/s) and pressure (ambient pressure) in two open air regions, sufficiently far away from the tunnel, so that the air flow itself was free to develop only because of the train movement. The ground and the tunnel walls were set as no slip and the train starting position was set in an open air region before the tunnel inlet.

4.2 Numerical results and flow analysis

As mentioned in Section 2 the vertical and lateral velocity components were negligible. Therefore, only the longitudinal component of the velocities, representing the primary influence of the slipstream velocity, will be shown also in the numerical results. The CFD accuracy is analyzed by considering wind histories generated by the train traveling in the even track direction, under matching measurement conditions of the experimental data (2.5 m from the center of the rails and 1.2 m above the platform).

The model's ability to replicate the air velocity created by the train was confirmed by assessing two distinct characteristics of the slipstream formed in tunnels: the piston wind and the counter-flow occurring in the annular space between the train and tunnel walls. As depicted in Figure 6 (a), the numerical model successfully simulates the speed up of the wind caused by the train entering the tunnel, commonly referred to as the piston effect. The flow generated by the piston effect is mailny one-dimensional

and is primarily influenced by the volume occupied by the train within the tunnel [5]. However, the representation of the piston effect is partially simplified due to the incompressible nature of the flow model; this simplification leads to a horizontal shift in the starting point of the air speed increase. Additionally, the differences in the profiles can be imputed also to geometric simplifications applied in the tunnel model near the entry section with respect to the real tunnel.

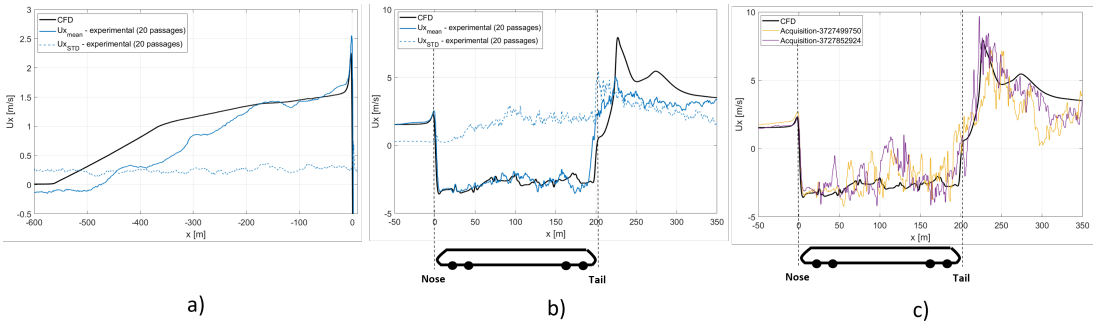

Figure 6: CFD results. In a) and b) the numerical air speed profile is compared with experimental ensemble air velocity before and during the train passage. In c) the comparison between two individual experimental time histories of train passages and the CFD results.

Regarding the airflow characteristics within the train area, specifically in the nose, boundary layer, and tail regions, Figure 6 (b) compares the profiles of longitudinal air speed between the simulated case and the ensemble of experimental curves. The simulated air speed profile effectively captures the peak at the nose and replicates the trend in the body region of the train where reverse flow conditions occur. Differencies in the growth of the boundary layer may arise from simplifications in the train model that does not include minor geometric details. In the boundary layer region between the nose and tail passage, as well as in the near-wake region, the CFD model does not perfectly reproduce the high-frequency variations in the airflow measured by the anemometers, which was expected using the URANS modeling method, since they provide a time-averaged representation of the flow. In evaluating the position and amplitude of the maximum velocity peak in the wake region, the ensemble mean experimental curve is found to be insufficient for the comparison. Therefore, in Figure 6 (c), the analysis is made correlating two individual time histories of train passages with the CFD results. This approach provides a more accurate representation, capturing not only the maximum peak value but also the overall trend effectively.

From the overall study, it can be inferred that the general trend of the slipstream and the characteristic air velocities along the entire length of the train are satisfactorily described. The CFD simulation can be further exploited to analyze the flow field not only in few measurement poins, as done in the experimental campaings, but to extend the analysis of the flow in all the platform region, understanding the air speed variations around the train and in different regions of the tunnel, where geometrical changes of its cross section are present.

Analyzing the annular region between the train body and the tunnel walls it is possible to visualize the train boundary layer growth, which in tunnels is limited by the counter flow of air generated by the piston effect, as shown in Figure 7, especially from the mid car of the train until the train end, where the train boundary becomes naturally larger.

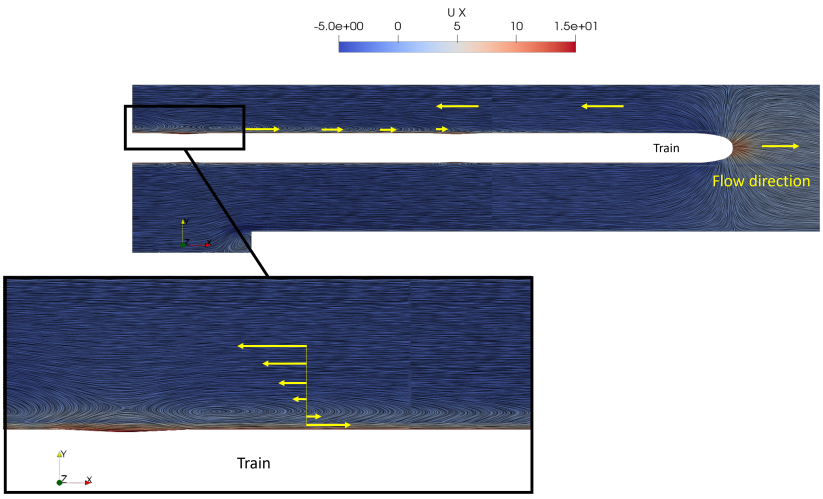

Figure 7: Train boundary layer growth and counter flow region. In the In the box the detail of the air flow inversion of direction near the train side is shown.

The magnitude of the piston wind directed towards the train end is dependent on the volume available between the train and the railway tunnel walls. To evaluate quantitatively this phenomenon it was chosen to acquire the slipstream velocity at three probes fixed on the platform at 2.5 m from the center of the track and 1.2 m high from the ground, in three regions with different volumes due to narrowing or widening of the platform, as shown in Figure 8, at two time intervals. The corresponding slipstream velocities are reported in Figure 9.

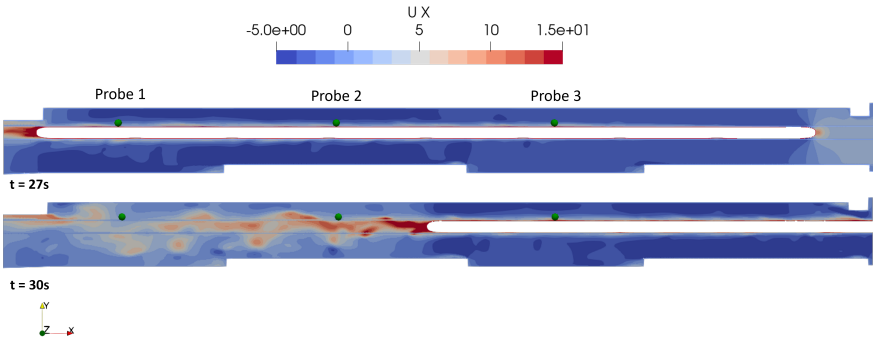

Figure 8: Slice at z=1.2m from the platform, representing the longitudinal air velocity (Ux) in the platform region when the train is passing. Three measurement probes are highlighted in green.

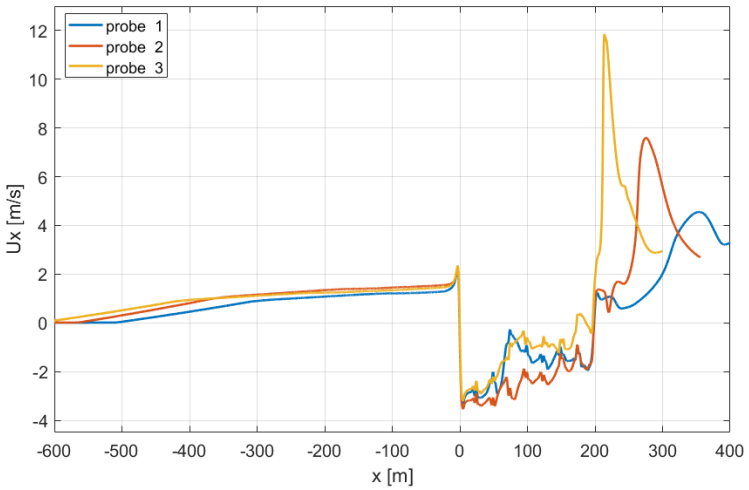

Figure 9: Comparison of three different probes placed on the even track platform. On x axis: train nose position from anemometer, on y axis: longitudinal air speed from the CFD simulation.

From the results, it can be drawn that in the boundaray layer area, the module of the counter flow velocity is proportional to the tunnel volume in each tunnel section, therefore probe n.2, which is located in a narrower region on the platform, measures a greater negative speed. Furthermore, the velocity maxima measured at the probes present a distribution in terms of amplitude and location after the tail passage, in the wake region; this variability is related to the position of the longitudinal vortices, typically generated after the train tail for high-speed trains, with respect to the measurement position, and reflects the behavior of the wind profiles measured during full-scale testing ([5]).

5 Conclusions

In this research, the results obtained though a full-scale experimental campaign carried out in open air and within a railway tunnel for the slipstream characterization of high speed train were described. In the second part of the study a numerical model includin the same train and tunnel geometries of the experimental campaign was introduced and the velocity results were compared with experimental data and used for considerations on the flow field generated in the platform. Referring to the analyses carried out in the previous sections, the following conclusions can be drawn.

The experimental campaign allowed to confirm the influence of the confined space on the air flow development and the typical differences between the slipstream generated in open air and in tunnels:

- In the nose region, the tunnel environment creates stronger wind peaks due to the piston effect and to the blockage effect given by the presence of the walls while in the boundary layer zone, between the train nose and tail, the most

characteristic difference between passages in open air and in confined space is the back flow generated by the train passage in the tunnel. Regarding the tail and wake region, the confinement effect is noticed for high-speed trains, where the tail related peaks present higher velocities for the tunnel environment, especially in the odd side, that has been proved to be the most critical due to the local tunnel geometry.

- In railway tunnels, the velocity difference between the back flow region and the maximum peak recorded in the near wake region could create discomfort and safety problems to passengers on the platform due to relevant air speed velocity variations. This strong variation is not recorded in open air, where the air speed is increasing in a monotonous trend up to the tail related peak.

The CFD simulations, carried out with a 3D, unsteady Reynolds-averaged Navier-Stokes approach, effectively replicates longitudinal air speed profiles in the train area, capturing trends in all the slipstream regions. Analyszing the numerical results, the folowing conclusions were drawn:

- The examination of the annular region between the train body and tunnel walls shows that the train boundary layer is constrained by the counter flow generated by the piston effect.
- The magnitude of the piston wind directed towards the train end is proportional to the tunnel volume, as measured from the CFD with three probes on the platform. This behavior is expected since the piston effect is mainly one-dimensional and depends on the train/tunnel blockage.
- Velocity maxima measured at probes in the wake region vary in amplitude and location, influenced by the position of longitudinal vortices generated after the train tail, which proves that the employed CFD model is able to reproduce the velocity distribution as in experimental measurements.

Acknowledgements

References

[1] D. Rocchi, G. Tomasini, P. Schito, and C. Somaschini. Wind effects induced by high speed train pass-by in open air. *Journal of Wind Engineering and Industrial Aerodynamics*, 173:279–288, 2018.

[2] D. Soper, C. Baker, and M. Sterling. Experimental investigation of the slipstream development around a container freight train using a moving model facility. *Journal of Wind Engineering and Industrial Aerodynamics*, 135:105–117, 2014.

[3] J. R. Bell, D. Burton, M. C. Thompson, A. H. Herbst, and J. Sheridan. Moving model analysis of the slipstream and wake of a high-speed train. *Journal of Wind Engineering and Industrial Aerodynamics*, 136:127–137, 2015.

[4] H. Hemida, C. Baker, and G. Gao. The calculation of train slipstreams using large-eddy simulation. *Proceedings of the Institution of Mechanical Engineers, Part F: Journal of Rail and Rapid Transit*, 228(1):25–36, 2014.

[5] S. Negri, G. Tomasini, P. Schito, and D. Rocchi. Full scale experimental tests to evaluate the train slipstream in tunnels. *Journal of Wind Engineering and Industrial Aerodynamics*, 240:105514, 2023.

[6] H. Hemida. Contribution of computational wind engineering in train aerodynamics—past and future. *Journal of Wind Engineering and Industrial Aerodynamics*, 234:105352, 2023.

[7] H. TSI. Technical specification for interoperability relating to the 'rolling stock'sub-system of the trans-European high-speed rail system. *Official Journal of the European Union L*, 847132, 2008.

[8] C. Standard. Railway applications-aerodynamics-Part 4: Requirements and test procedures for aerodynamics on open track. *CEN EN14067-4*, 2009.

[9] C. Standard. Railway applications-aerodynamics-Part 5: Requirements and test procedures for aerodynamics in tunnels. *CEN EN14067-5*, 2009.

[10] C. J. Baker, A. Quinn, M. Sima, L. Hoefener, and R. Licciardello. Full-scale measurement and analysis of train slipstreams and wakes. Part 1: Ensemble averages. *Proceedings of the Institution of Mechanical Engineers, Part F: Journal of Rail and Rapid Transit*, 228(5):451–467, 2014.

[11] W.-h. Li and T.-h. Liu. Three-dimensional characteristics of the slipstream induced by a high-speed train passing through a tunnel. *DEStech Transactions on Engineering and Technology Research*, pages 502–512, 2017.

[12] T. Gilbert, C. Baker, and A. Quinn. Gusts caused by high-speed trains in confined spaces and tunnels. *Journal of wind engineering and industrial aerodynamics*, 121:39–48, 2013.